MHD Simulation of Multi-pulsed Helicity Injection in High-*q* ST Plasmas

Takashi Kanki[1], Masayoshi Nagata[2], Yasuhiro Kagei[3]

[1]*Japan Coast Guard Academy,* [2]*University Hyogo,* [3]*RIST*

17th Numerical Experiment of Tokamak (NEXT) Meeting
University of Tokyo, Kashiwa, Japan, 15-16 March 2012

Helicity-driven spherical system

Many experiments on the **coaxial helicity injection** (CHI) using a magnetized coaxial plasma gun (MCPG) have been carried out for **spherical torus** (ST) to understand the mechanism of current drive or MHD relaxation.

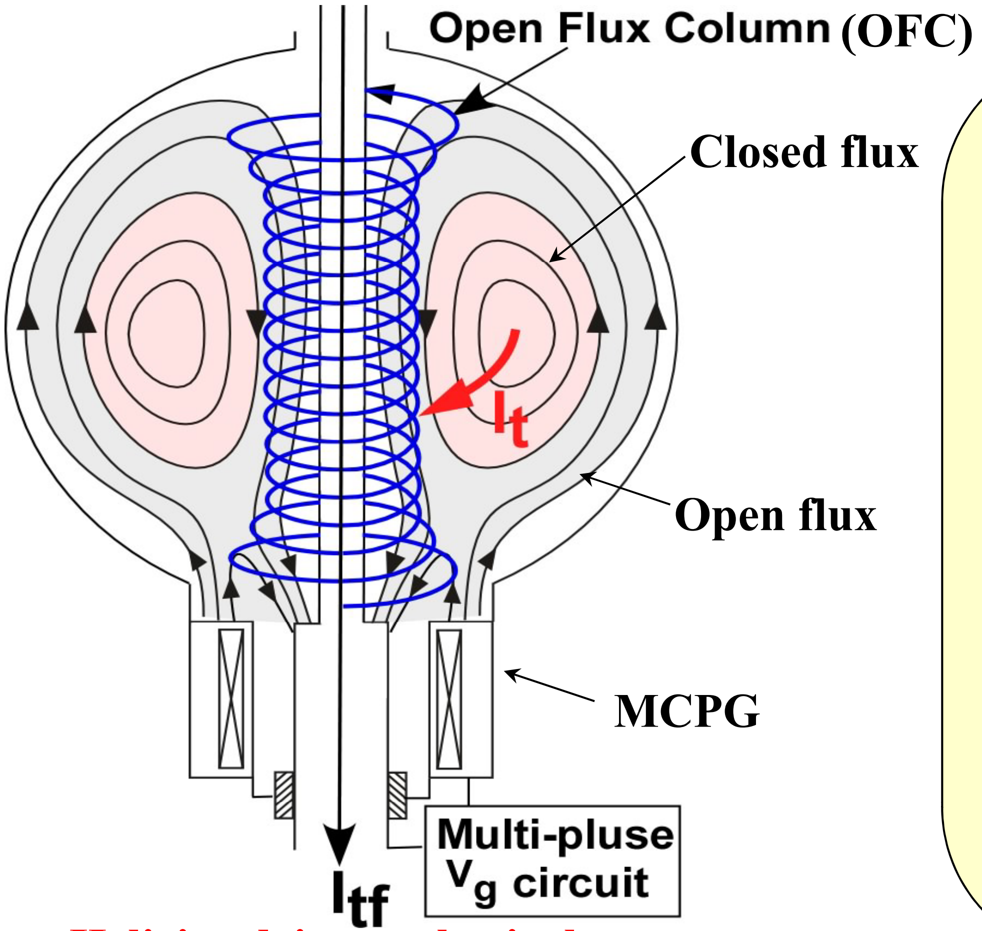

Helicity-driven spherical system

-- Formation and sustainment of the ST configuration by CHI are considered to be due to an ***n*=1 kink mode** driven by the OFC.

-- This mode converts injected toroidal flux into poloidal flux, resulting in an **flux amplification** which involves **magnetic reconnection events**. In the driven phase, the events open magnetic surfaces and deteriorate **energy confinement**.

-- In the decay phase after the driven phase, the magnetic fluctuations become small, **allowing closed flux surfaces to form, resulting in good confinement.**

Multi-pulsed CHI (M-CHI) scheme

1. Driven phase: Current drive is performed with allowing the deterioration of confinement.
2. Decay phase : Closed flux surfaces are formed, resulting in good confinement.

↓

The M-CHI scenario aims to achieve simultaneously a quasi-steady sustainment and good confinement by repeating the driven and decay phases.

The purpose of this study is to perform the 3-D nonlinear MHD simulations to investigate the dynamics of the magnetic field structure and plasma flows generated during the M-CHI in the high-*q* ST (*q*>1).

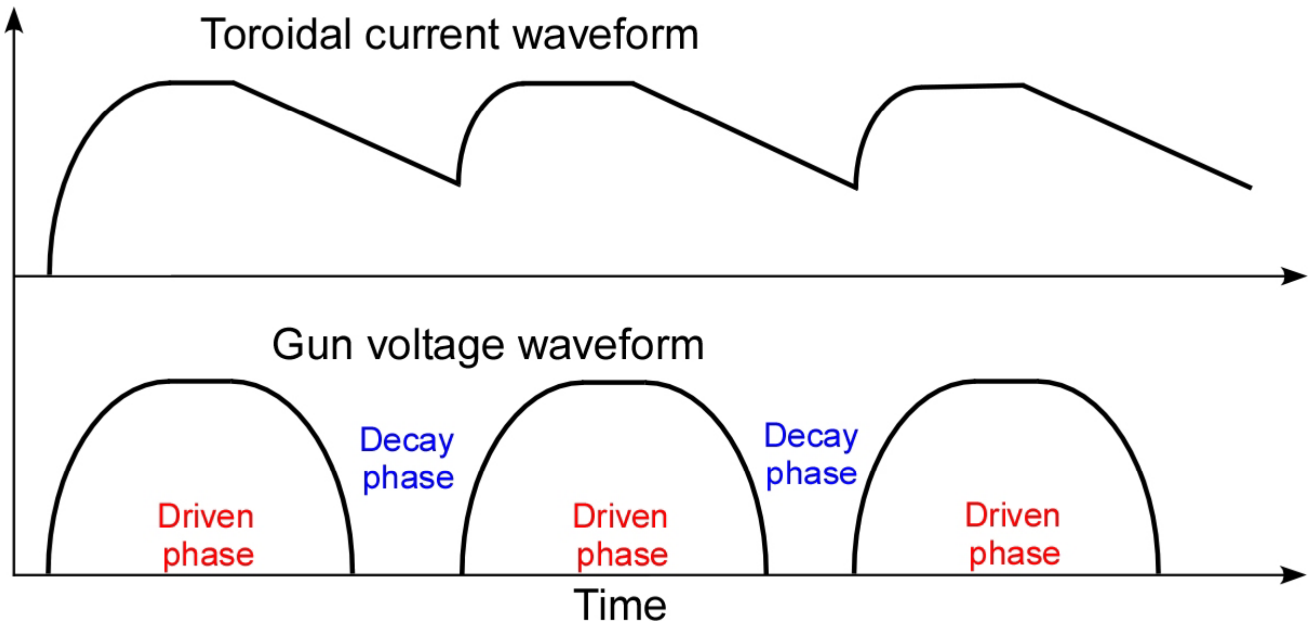

HIST device and double-pulsing CHI

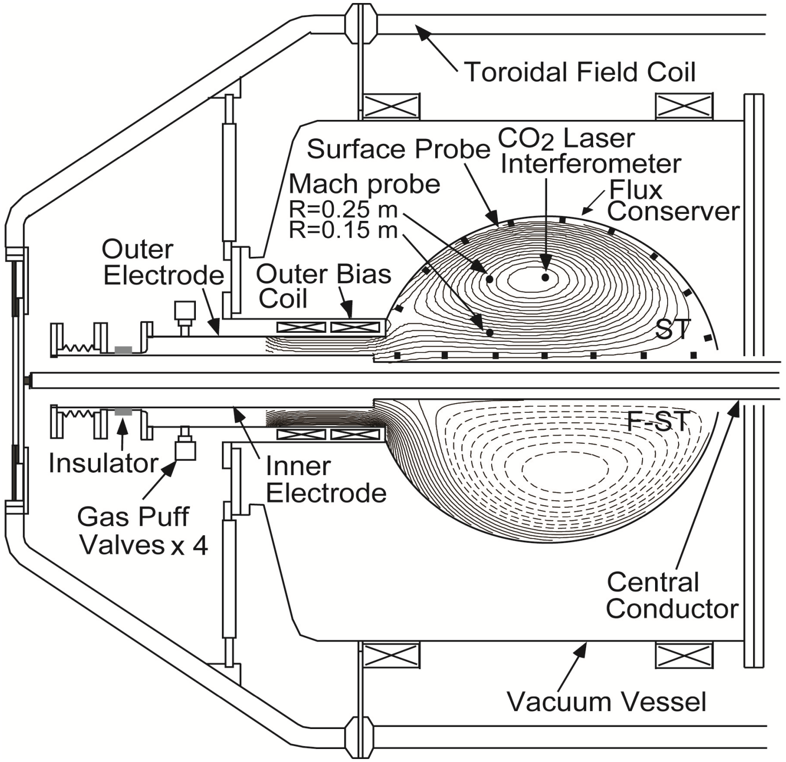

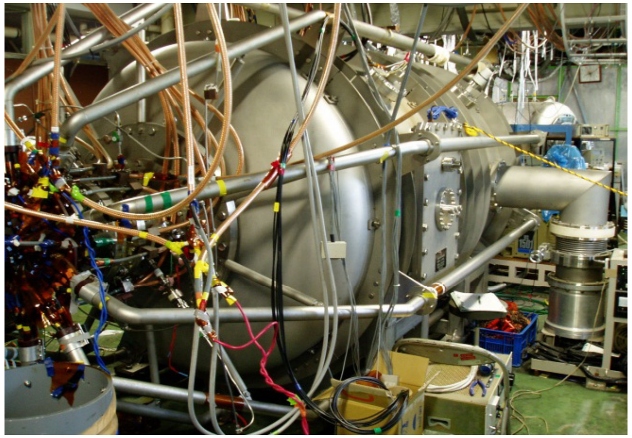

- **HIST plameters**

  R=0.3 m, a=0.24 m , A=1.25

  n_e=0.5-1 x 10^{20} m^{-3}

  T_e, T_i = 10-40 eV

  I_t< 150 kA, $h_e=\omega_{ce}\tau_{ie}$=50-200

  $S^*=R/l_i$~10 $l_i=(c/\omega_{pi})$=2~3 cm

- **TF coil current**

  Spheromak, Low-q ST: q ~ I_{tf} (= 0-30 kA) / I_t<1

  High-q ST: q ~ I_{tf}(= ~ 150 kA) / I_t>1

- **Power supply system for double-pulse**

  Formation capacitor banks

  V = 3-10 kV, C = 0.6 mF

  Injection current : I_g ~ 30 - 60 kA

- **Sustainment capacitor banks**

  First pulse : V < 900 V, C = 336 mF

  Second pulse : V < 900 V, C = 195 mF

2nd pulse voltage : V_g ~ 400 V 2nd pulse current : I_g ~ 10-20 kA

Double pulsing CHI discharge (High-q)

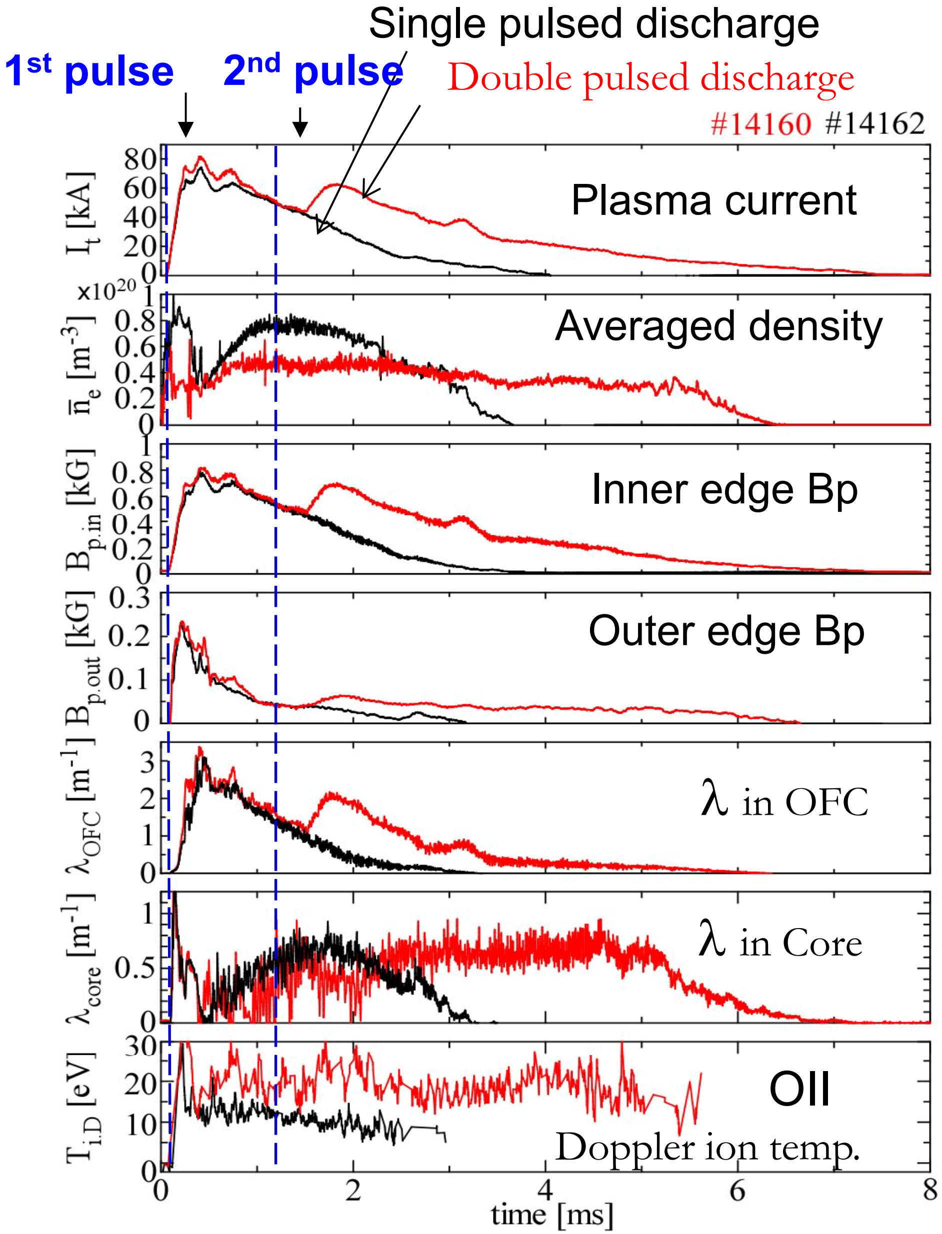

- By secondly pulsing the MCPG at t = 1.5 or 2.5 ms during the partially decay phase, total plasma current is effectively amplified against the resistive decay. The core current density is generated due to dynamo.
- The sustainment time has increased up to 6 -8 ms which is longer than that in the single CHI case.
- The edge λ in the OFC is larger than the core λ , causing helicity transport.

$$\lambda = \mu_0 I_{t.} / \Psi_t$$

- Ion Doppler temperature increases from 20 eV up to 30 eV.

Flows and density profiles

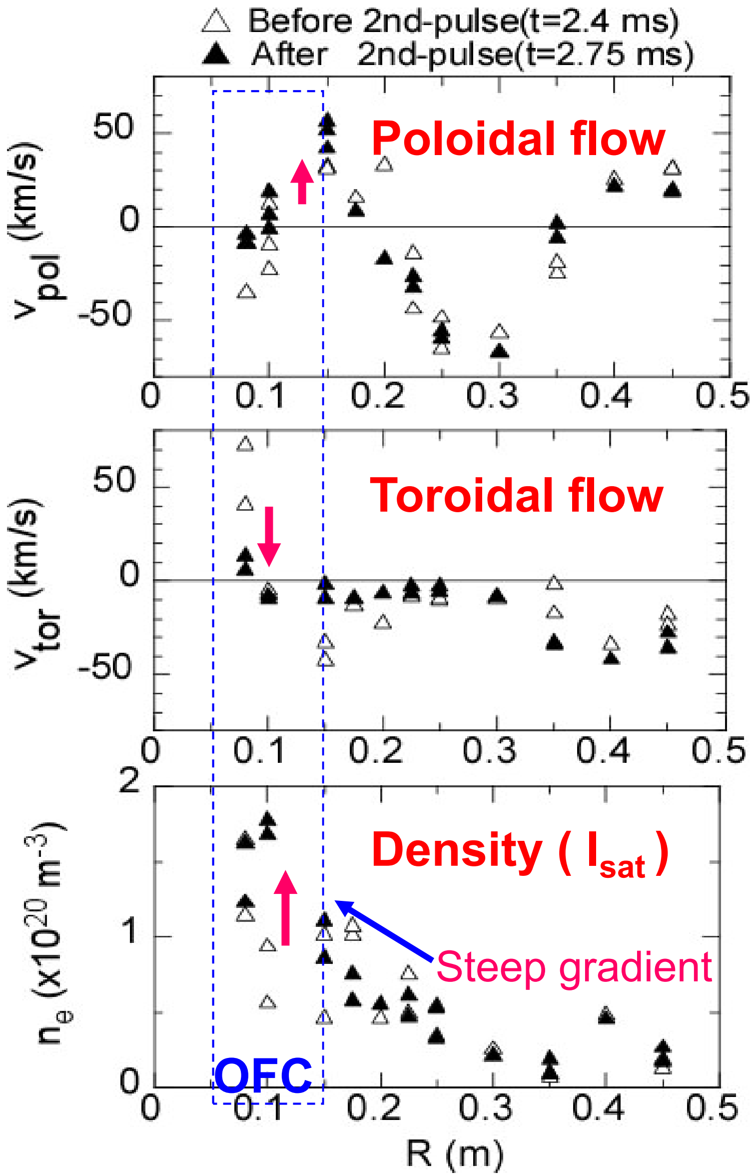

$$v_p = \frac{E_r \times B_t}{B^2} - \boxed{\frac{\nabla p_i \times B_t}{enB^2}}$$

⇩

Poloidal shear flow

Diamagnetic current

⇨ Diamagnetic properties of OFC

Radial electric field E_r

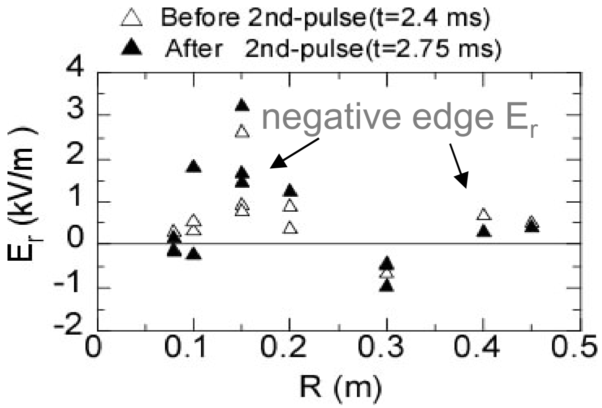

$$E_r \approx \frac{\nabla p_i}{en_i Z_i} \boxed{-(v_p B_t} - v_t B_p)$$

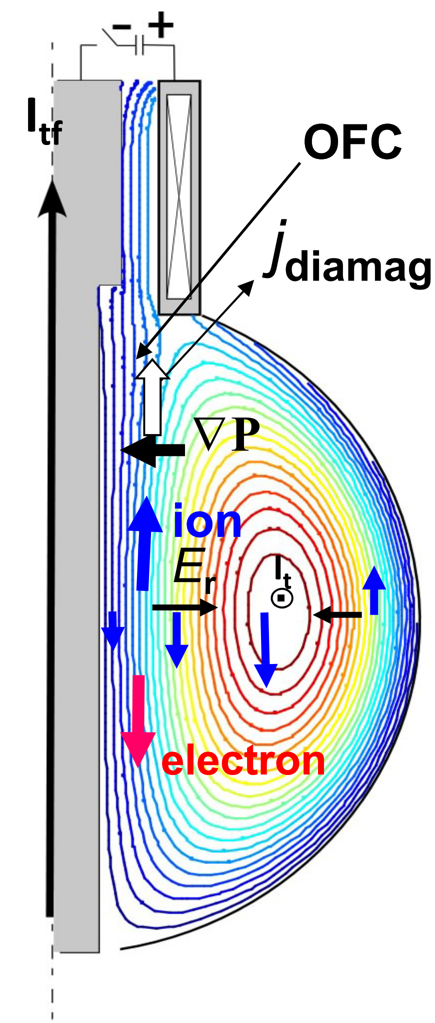

Radial profile of dynamo electric field

$$< \tilde{v} \times \tilde{B} >_{\parallel} - < \tilde{j} \times \tilde{B} >_{\parallel} /en$$

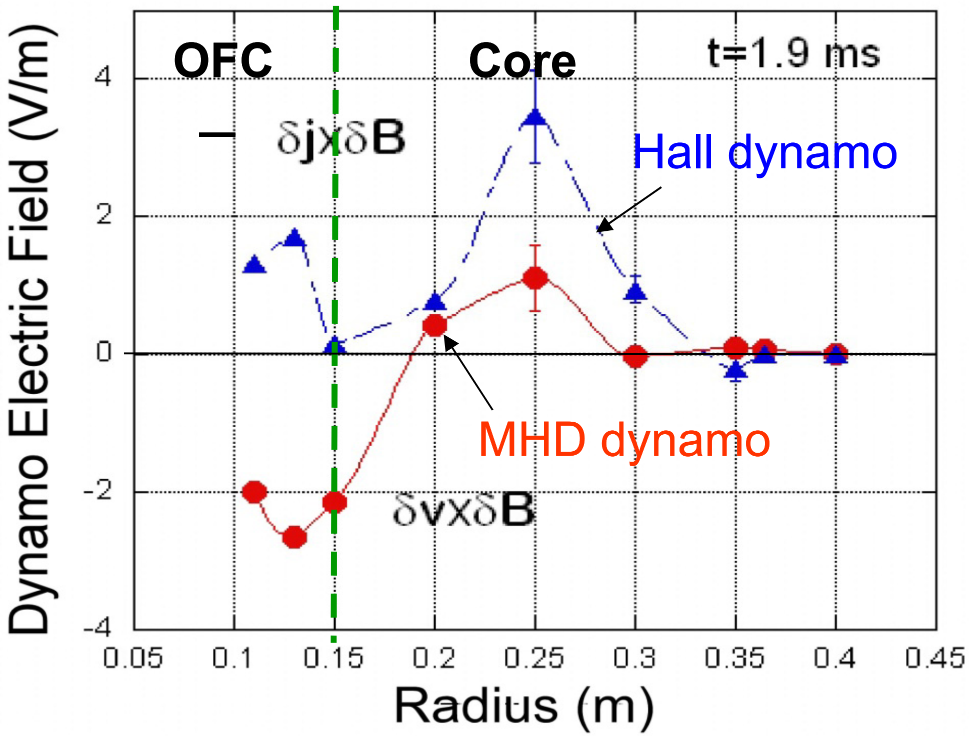

Collisional drag of electrons on the ions accelerates the ions in the core.

Electrons become slow down due to anti-dynamo E_{MHD}

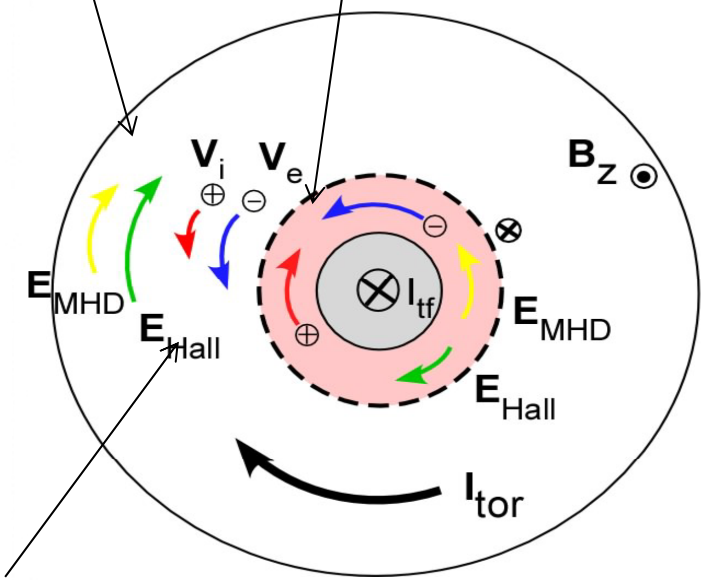

Ions are accelerated due to E_{Hall} in the direction of the current in the OFC.

Anti-MHD dynamo

- Hall dynamo driven current in the OFC is the same direction as the mean current.
- MHD anti-dynamo electric field in the OFC reduces the mean current.

⇨ Electron locking model [1]

$$\delta\omega_{ce}\tau_{ie} > \delta/R$$

[1] T.R. Jarboe *et al.*, Nucl. Fusion **51** 063029 (2011).

Nonlinear resistive MHD equations

$$\frac{\partial \rho \mathbf{v}}{\partial t} = -\nabla \cdot \rho \mathbf{v}\mathbf{v} + \mathbf{j} \times \mathbf{B} - \nabla p - \nabla \cdot \overleftrightarrow{\mathbf{\Pi}} \qquad \textbf{(1)}$$

$$\frac{\partial \mathbf{B}}{\partial t} = -\nabla \times \mathbf{E} \qquad \textbf{(2)}$$

$$\frac{\partial p}{\partial t} = -\nabla \cdot \left(p\mathbf{v} - \kappa \nabla T\right) - (\gamma - 1)\left(p \nabla \cdot \mathbf{v} + \overleftrightarrow{\mathbf{\Pi}} : \nabla \mathbf{v} - \eta j^2\right) \qquad \textbf{(3)}$$

$$\mathbf{E} = -\mathbf{v} \times \mathbf{B} + \eta \mathbf{j} \qquad \textbf{(4)}$$

$$\mathbf{j} = \nabla \times \mathbf{B} \qquad \textbf{(5)}$$

$$T = p / \rho \qquad \textbf{(6)}$$

$$\overleftrightarrow{\mathbf{\Pi}} = \nu \left(\frac{2}{3} (\nabla \cdot \mathbf{v}) \overleftrightarrow{\mathbf{I}} - \nabla \mathbf{v} - {}^{t}(\nabla \mathbf{v}) \right) \qquad \textbf{(7)}$$

ρ : Spatially and temporally constant

Spatial derivatives: The second-order finite differences method
Time integration: The fourth-order Runge-Kutta method

Simulation region and boundary condition

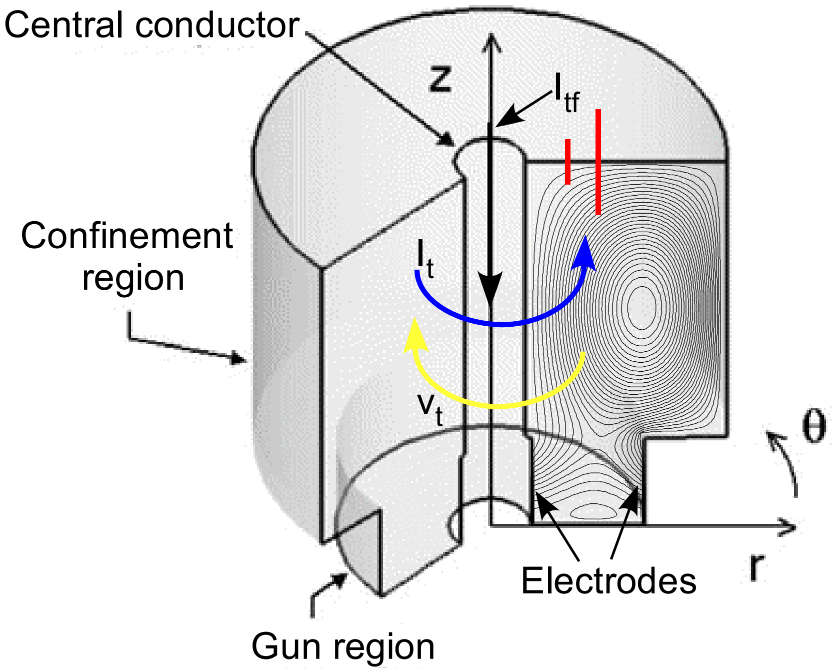

Confinement region

$$0.15L_r \le r \le L_r\,,\ 0.5L_r \le z \le 2L_r$$
$$N_r \times N_\theta \times N_z = 69 \times 64 \times 121$$

Gun region

$$0.175L_r \le r \le 0.65L_r\,,\ 0 \le z < 0.5L_r$$
$$N_r \times N_\theta \times N_z = 39 \times 64 \times 40$$

Boundary condition

Velocity

$$\boldsymbol{v} = 0$$

Magnetic field

$$\boldsymbol{B}_\perp = \begin{cases} 0; & \text{All boundaries except for electrode surfaces} \\ \text{Non-zero}; & \text{Electrode surfaces} \end{cases}$$

$$\frac{\partial \boldsymbol{B}_\perp}{\partial t} = 0$$

Bias field is temporally constant.

Electric field External electric field E_{inj}

$$\mathbf{E} = \begin{cases} 0; & \text{All boundaries except for the gap between electrodes} \\ E_r \text{ of non-zero}; & \text{Gap between electrodes} \end{cases}$$

Heat flux can passes across the all boundaries.

Initial condition

Numerical axisymmetric MHD equilibrium with finite pressure

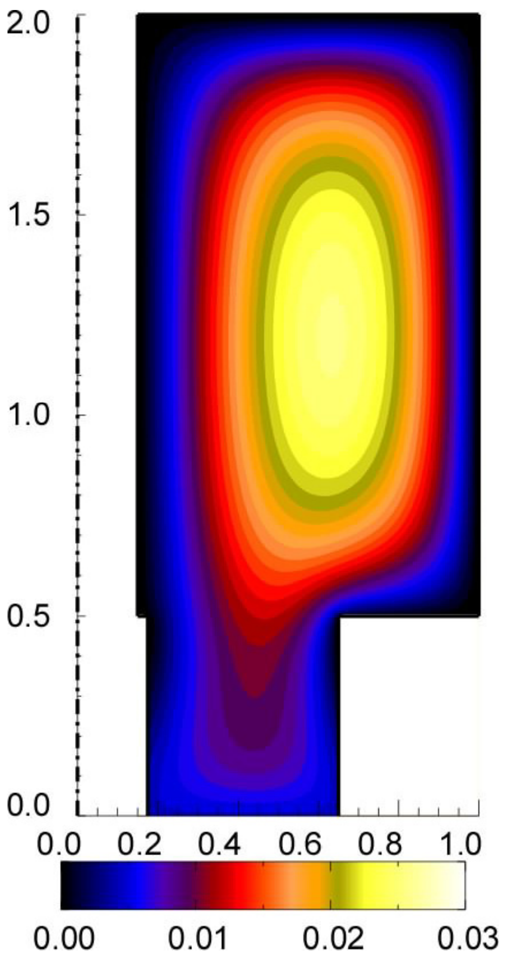

Poloidal flux contour

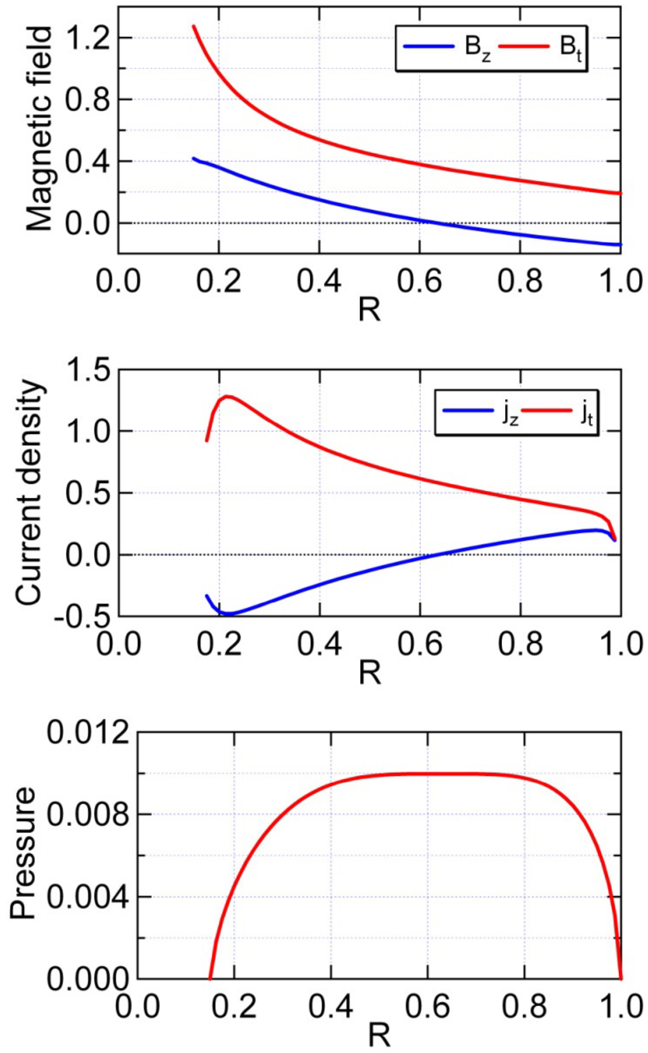

Radial profile

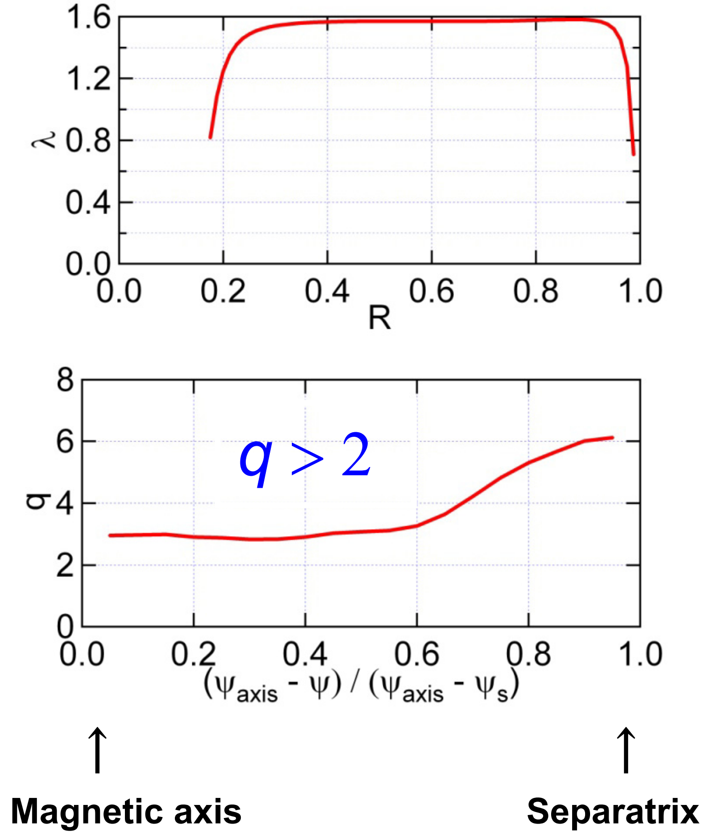

Safety factor

Parameters

Parameters	Normalized quantities	Real quantities
Radius of confinement region L_r	1.0	0.5 m
Number density n_0	1.0	5.0×10^{19} /m^3
Characteristic magnetic field B_0	1.0	0.2 T
Initial toroidal current I_t	1.0	80 kA
Initial temperature T	1.0×10^{-2}	40 eV
External radial electric field E_{inj}	1.0×10^{-2}	1.3 kV/m
TF current I_{tf}	1.2	96 kA
Initial parallel current density on axis λ_{axis}	1.6	3.2 /m
Resistivity η	2.0×10^{-4}	7.8×10^{-5} $\Omega\cdot$m
Viscosity ν	1.0×10^{-3}	2.6×10^{-5} kg/m·sec
Conductivity κ	1.0×10^{-3}	0.32 W/m·K
Alfven time τ_A	1.0	0.81 μsec

Alfven velocity $v_A \sim 620$ km/s, Magnetic Reynolds number $S \sim 5000$

Time evolution of external electric field, toroidal current, poloidal flux, and magnetic energy for each toroidal Fourier mode *n*

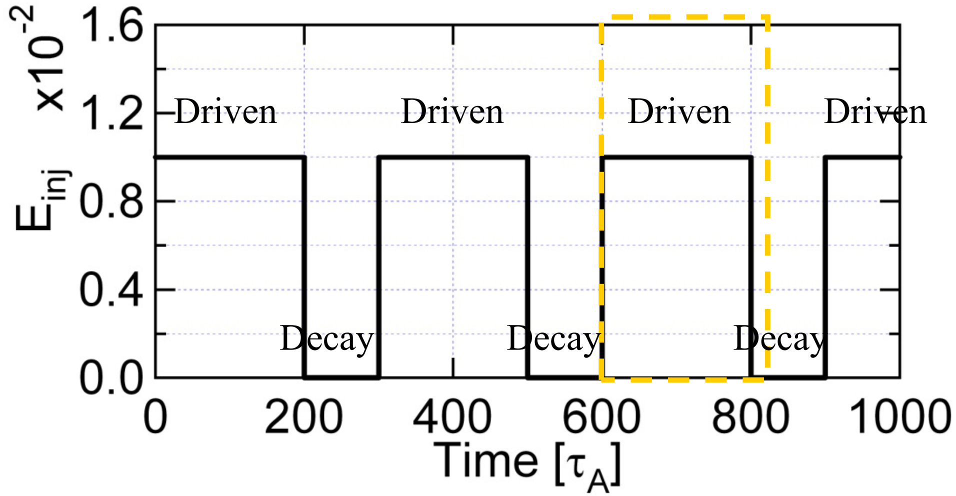

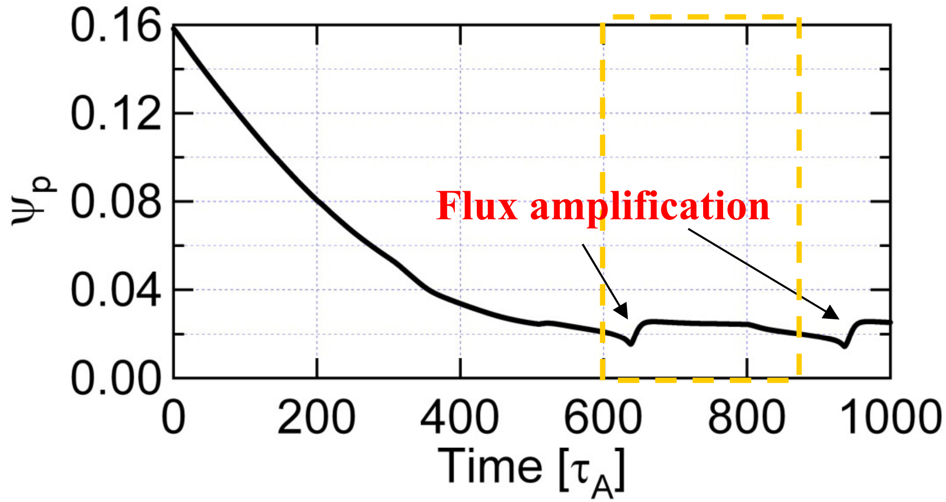

The external electric field is applied in the shape of periodic pulses.

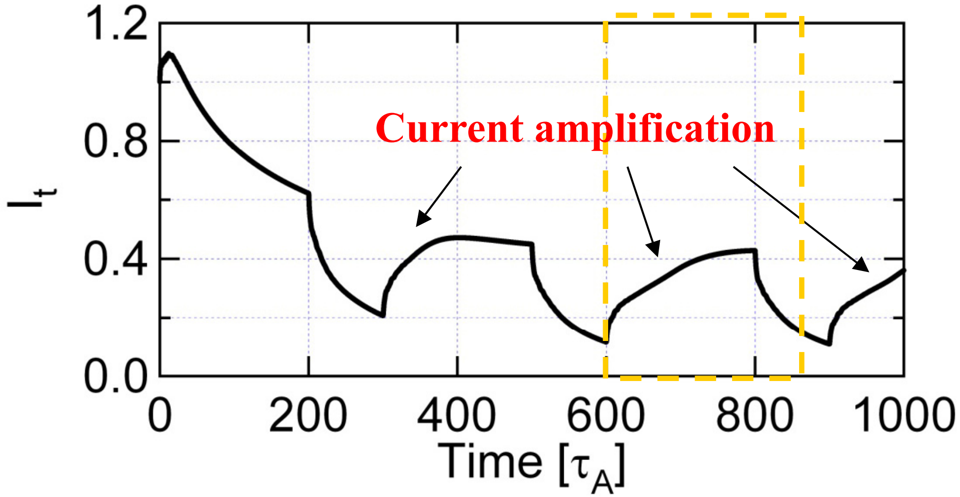

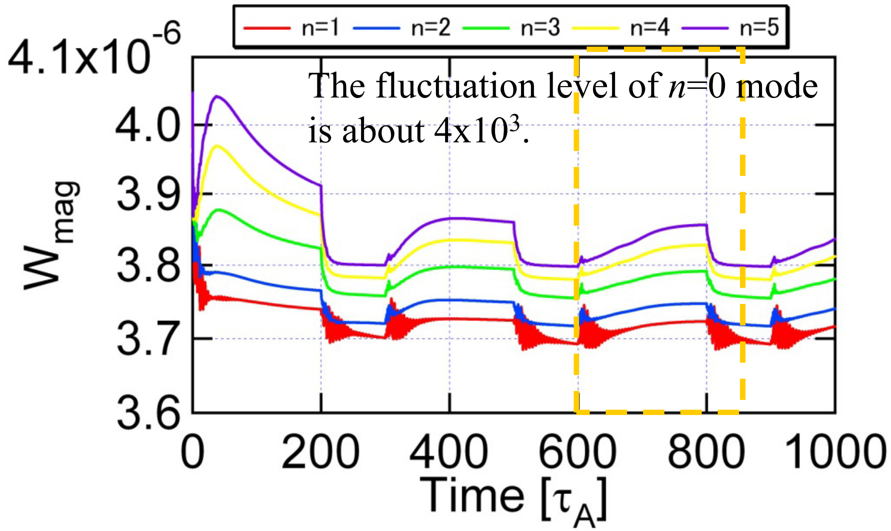

-- The toroidal current is amplified against the resistive decay during the driven phase.

-- The flux amplification is not observed just after $t=300\tau_A$ because the plasmoid can not be ejected due to the magnetic pressure of pre-existing ST.

-- The n=0 mode is dominant, and configuration is almost axisymmetric.

Polarity of toroidal current and flow

Poloidal cross section on θ=0 plane

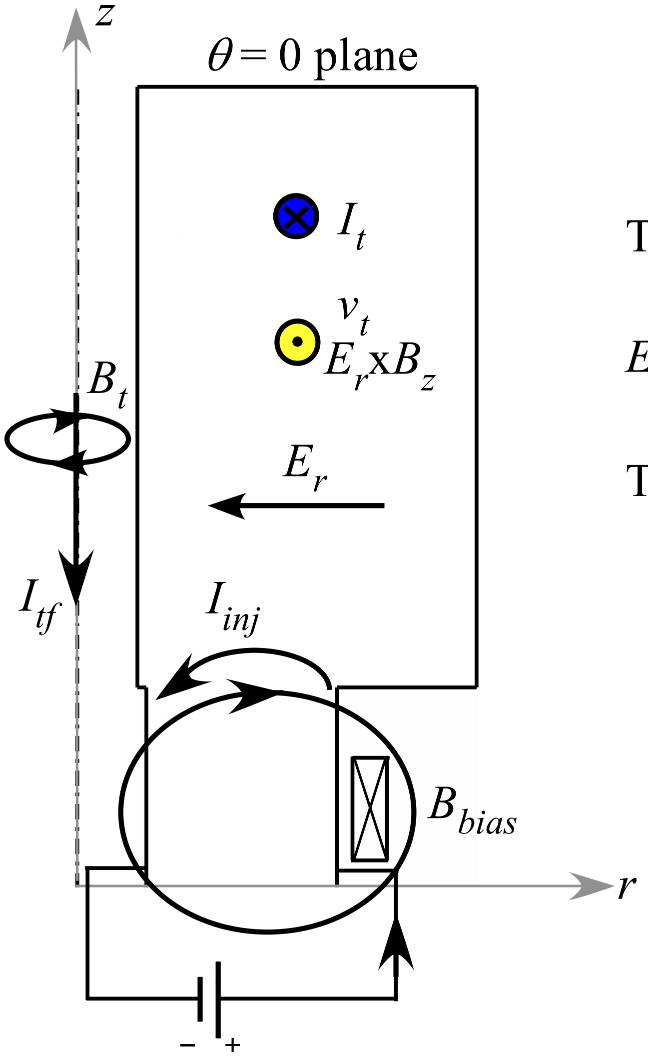

Toroidal current I_t ⊗

ExB drift rotation v_d ⊙

Toroidal flow v_t ⊙

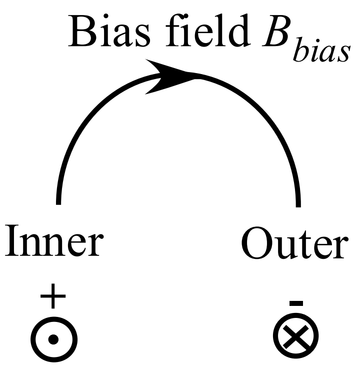

View of toroidal cross section
from opposite direction to the gun

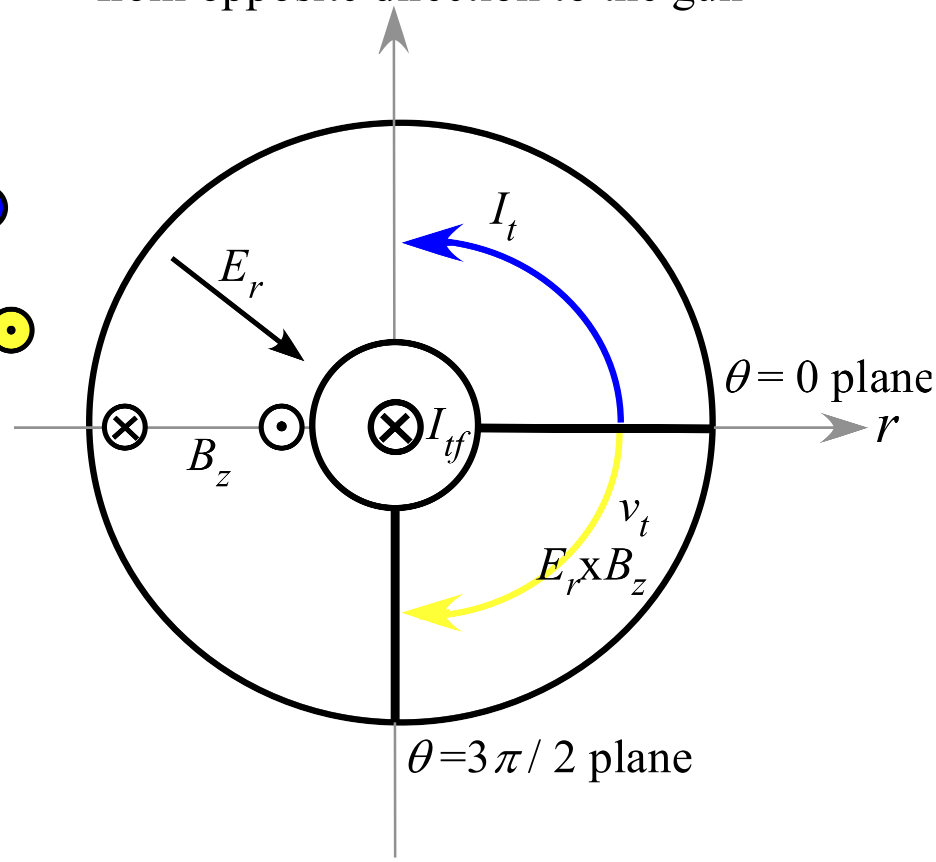

The direction of *E*x*B* drift rotation is based on the outer side of the bias field.

Time evolution of poloidal field on poloidal cross section

Driven phase

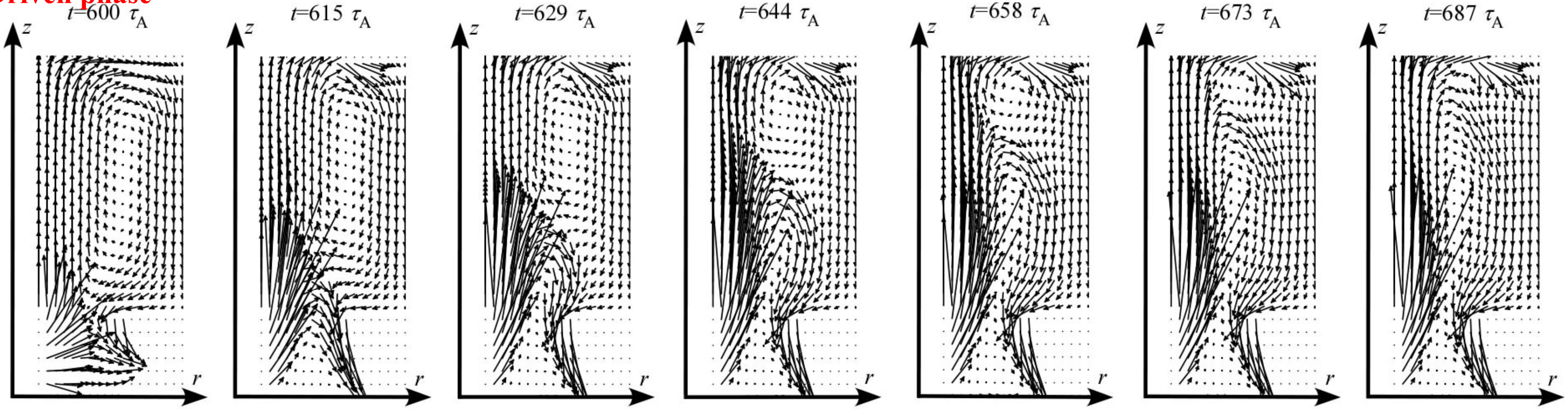

The plasmoid is ejected from the gun region due to the Lorentz force, and is then merged with the pre-existing ST. As the result, the poloidal flux amplification occurs.

E_{inj}=0 (Decay phase)

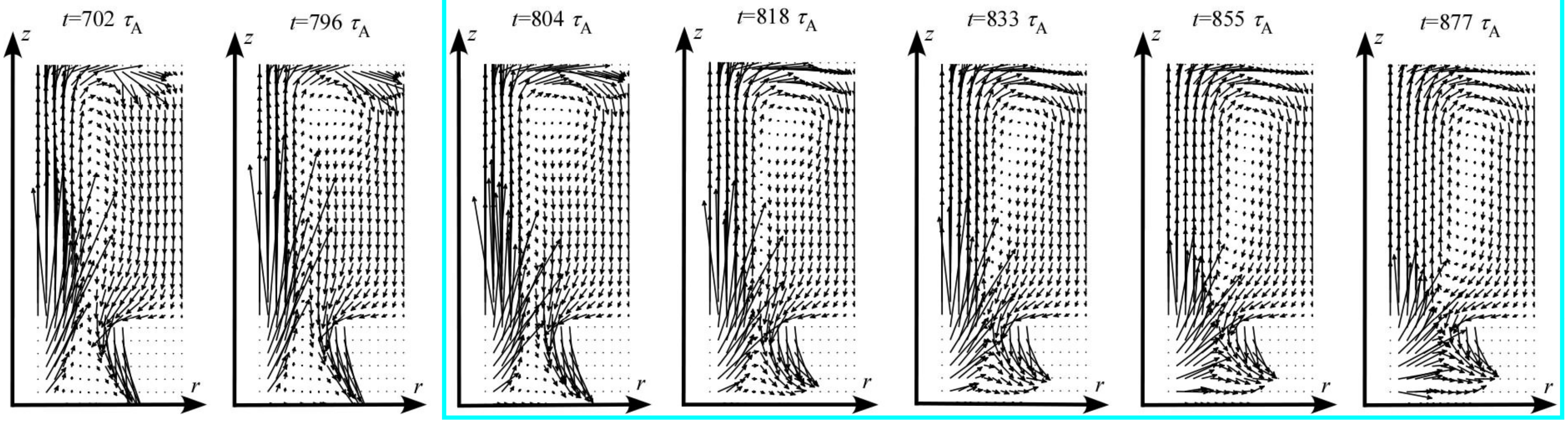

The closed flux surfaces are rebuilt due to the dissipation of the magnetic fluctuation in the COFC.

Time evolution of flows on poloidal cross section

Driven phase

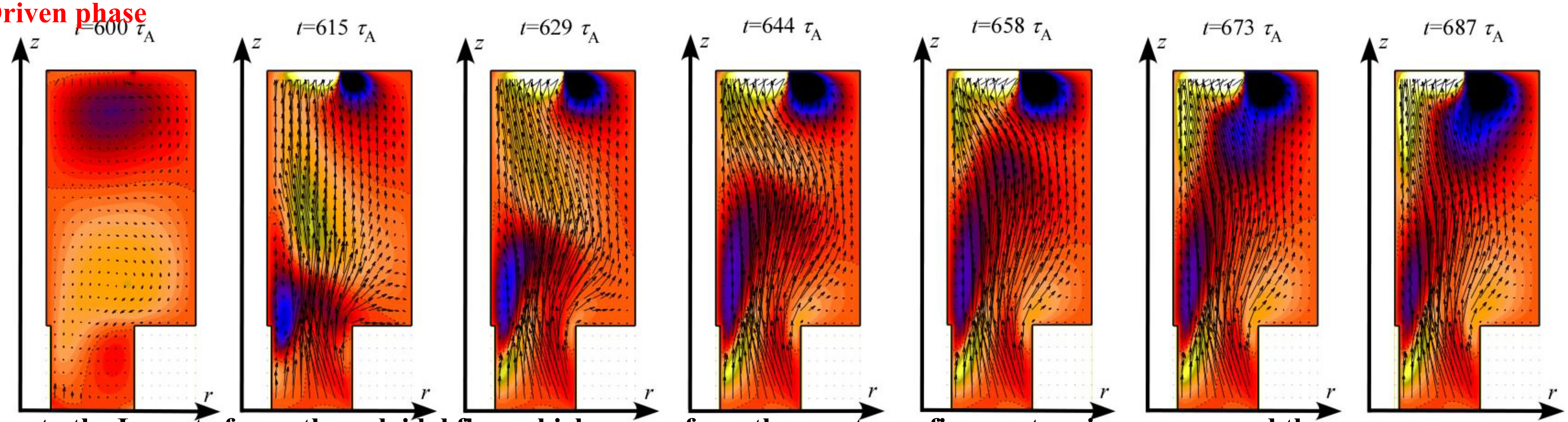

Due to the Lorentz force, the poloidal flow which moves from the gun to confinement region occurs, and the blue toroidal flow is driven in the same direction as the toroidal current.

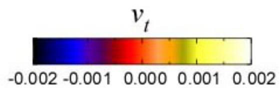

The blue toroidal flow is caused by the Lorentz force based on the diamagnetic current.

E_{inj}=0 (Decay phase)

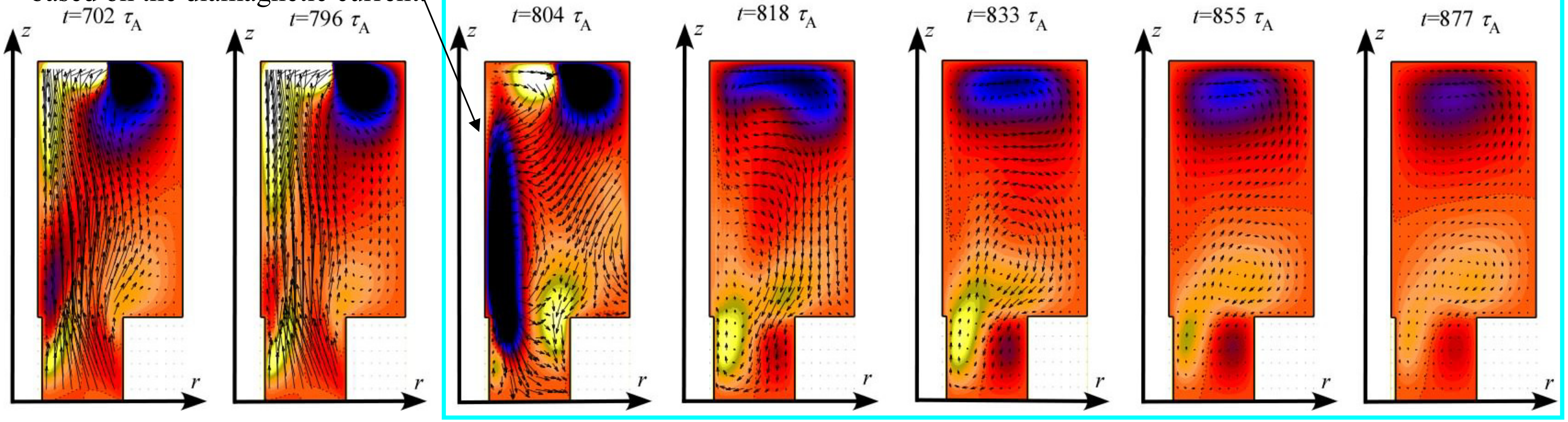

At t=804τ_A, the poloidal flow which moves from the confinement to gun region is induced due to the pressure gradient.

Time evolution of λ profiles on poloidal cross section

Driven phase

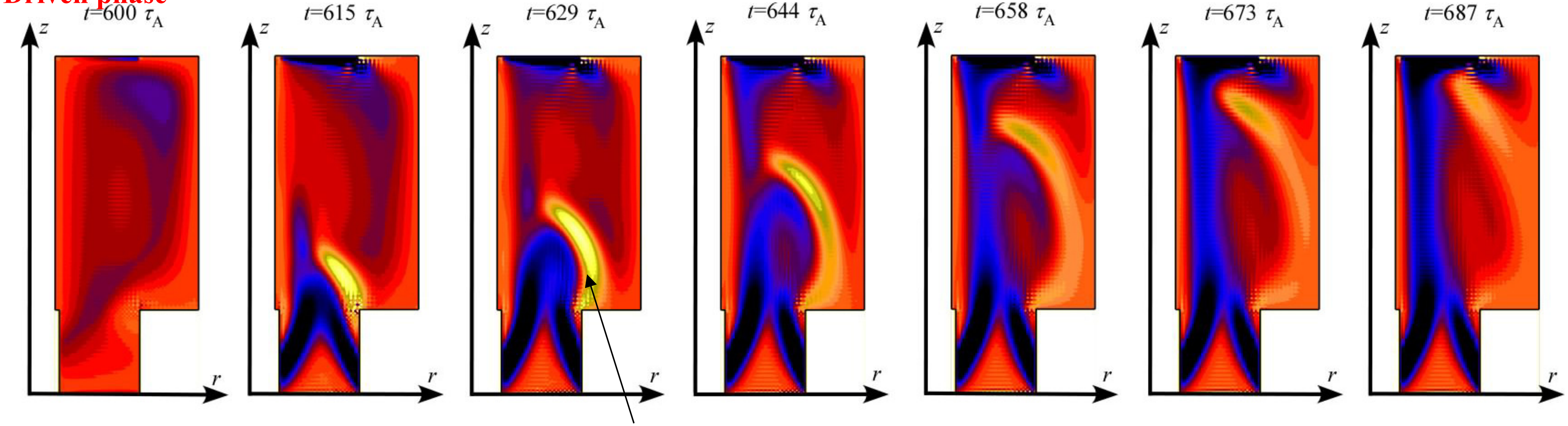

The current sheet is caused by approach of the anti-parallel magnetic field lines during the plasmoid ejection.

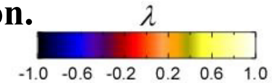

E_{inj}=0 (Decay phase)

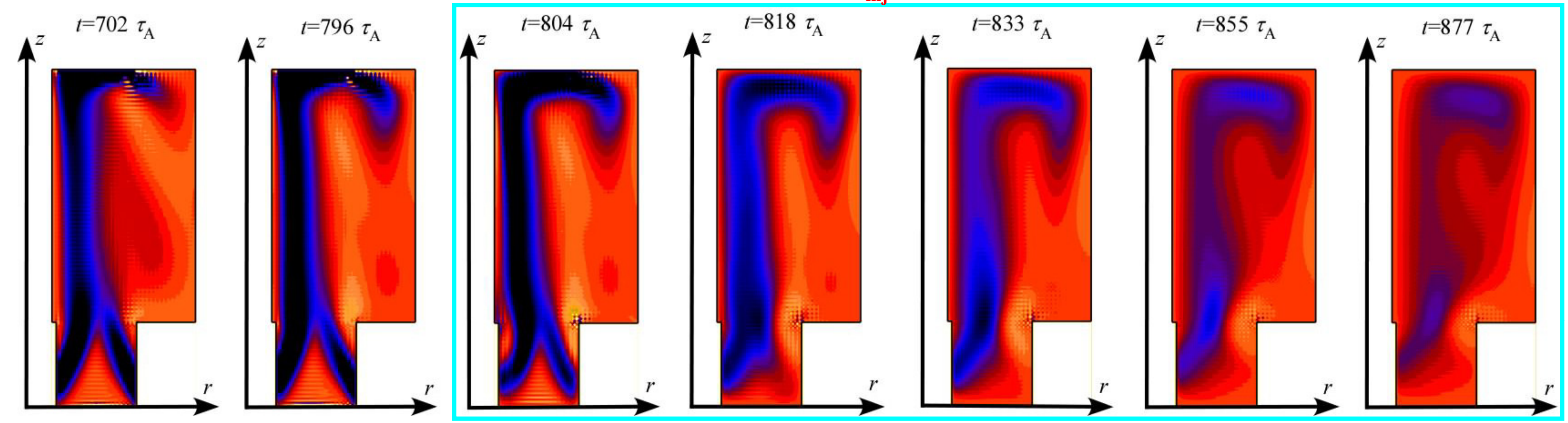

The λ concentrated in the COFC region is diffused to core region, approaching the Taylor state.

Time evolution of pressure profiles on poloidal cross section

Driven phase

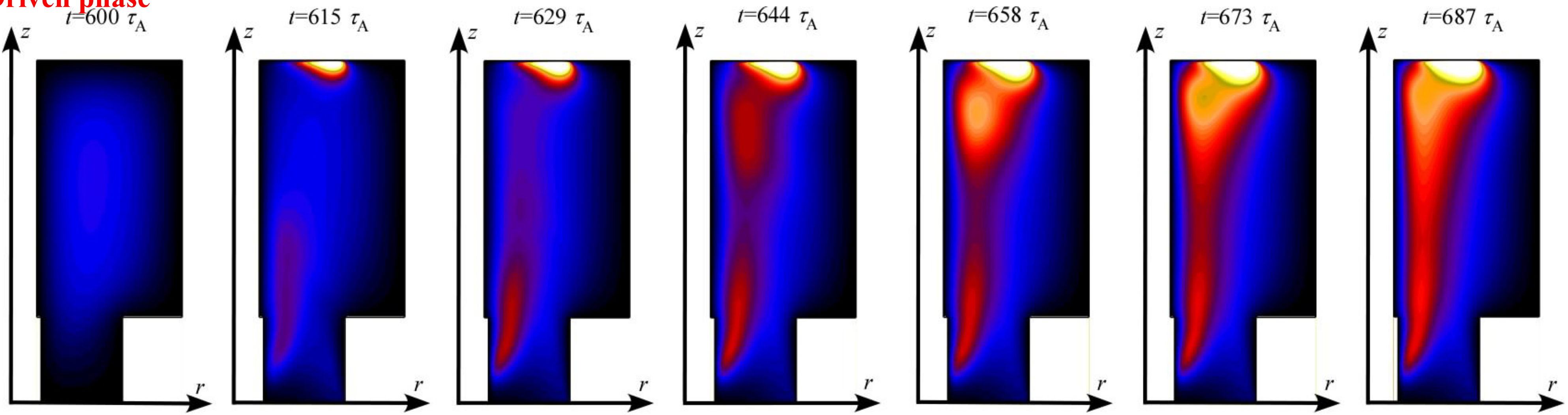

The Ohmic heating is caused by the concentration of the current density through the electric field at the gap and the ejected plasmoid.

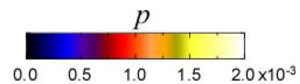

E_{inj}=0 (Decay phase)

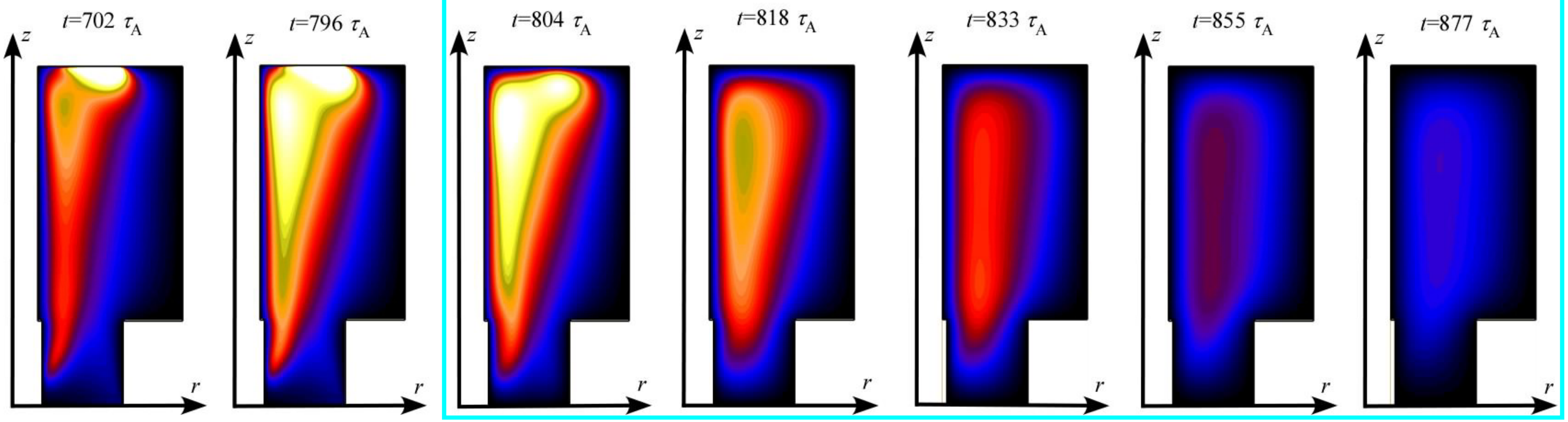

The broad pressure profile is formed in the core region due to the diffusion of pressure from the COFC to core region.

Time evolution of radial electric field on toroidal cross section

Driven phase

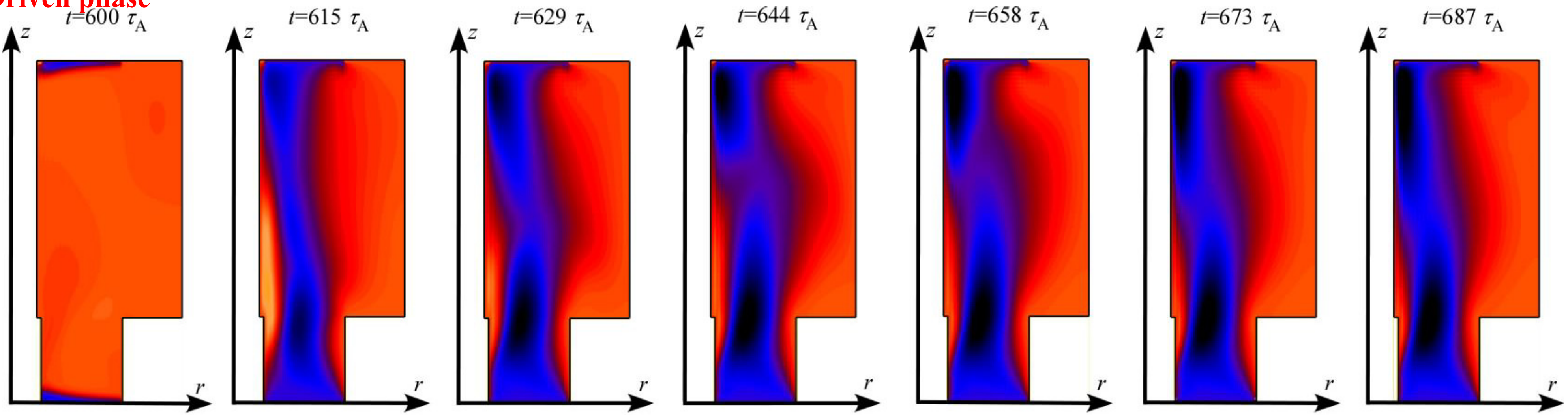

The negative electric field which has the same polarity as the external electric field exists in the COFC.

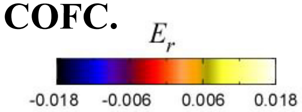

E_{inj}=0 (Decay phase)

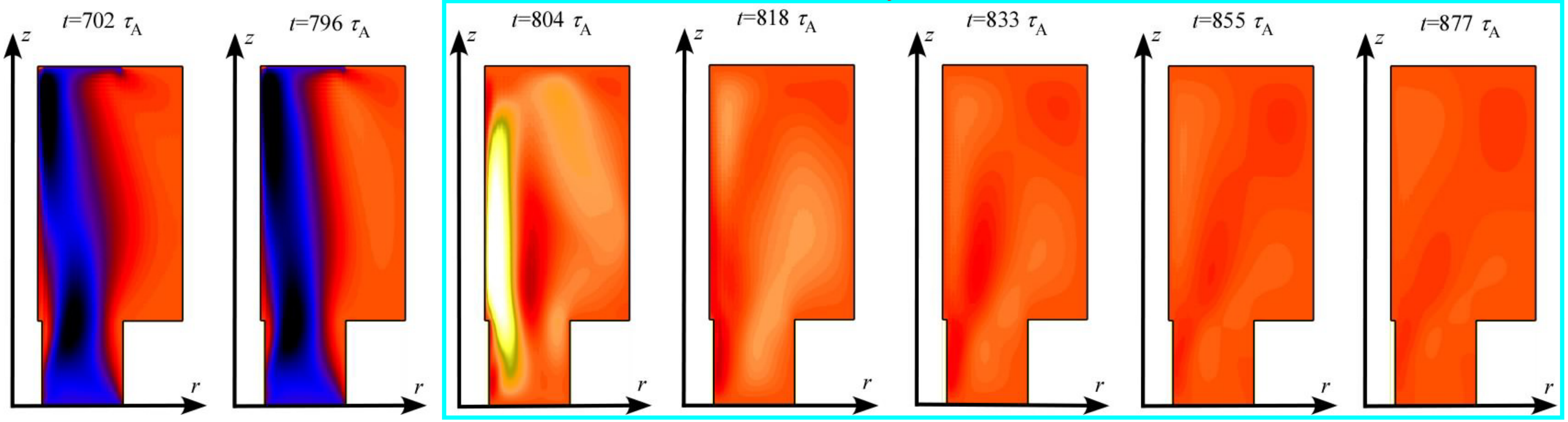

The current density is diffused from the COFC to core region due to the positive electric field in the COFC.

Time evolution of MHD dynamo on poloidal cross section

Driven phase

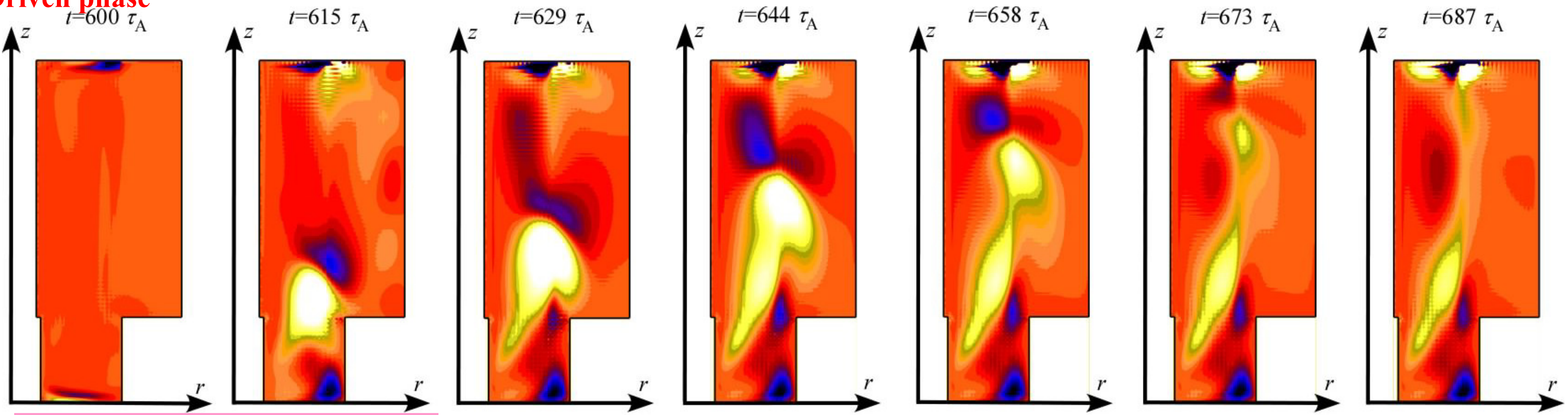

$$\text{Dynamo}: \quad \overline{E}_{/\!/} < \eta\,\bar{j}_{/\!/}, \text{ i.e., } \left\langle \tilde{\boldsymbol{v}} \times \tilde{\boldsymbol{B}} \right\rangle_{/\!/} > 0$$

$$\text{Antidynamo}: \quad \overline{E}_{/\!/} > \eta\,\bar{j}_{/\!/}, \text{ i.e., } \left\langle \tilde{\boldsymbol{v}} \times \tilde{\boldsymbol{B}} \right\rangle_{/\!/} < 0$$

The α dynamo effect represents an electromotive force generated by turbulence in the direction along the mean magnetic field.

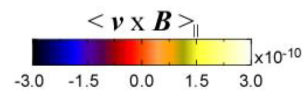

E_{inj}=0 (Decay phase)

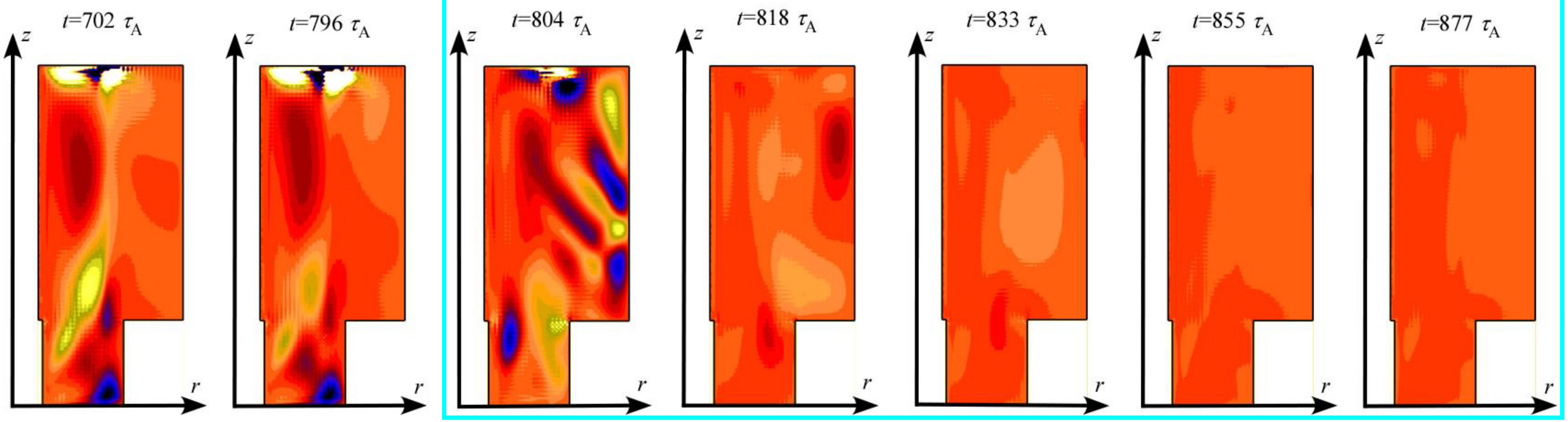

During plasmoid ejection process, the dynamo effect which diverts power from the gun to core region is observed.

Summary

We carried out the nonlinear MHD simulation of the current drive of **high-*q* ST** plasmas by the **M-CHI**.

1. During the driven phase, the poloidal flux and the toroidal current are amplified by **the axisymmetric merging of the pre-existing ST plasma with ejected one**.

2. During the decay phase, the **ST approaches the axisymmetric MHD equilibrium state without flow** due to the dissipation of magnetic fluctuations to **rebuild the closed flux surfaces**.

3. **The positive electric field** in the COFC causes **the current density or λ to diffuse from the COFC to core region**, leading **the helicity transport**.